nature protocols

PROTOCOL

https://doi.org/10.1038/s41596-019-0160-8

High-resolution 3D imaging of fixed and cleared organoids

Johanna F. Dekkers[1,2,3,4], Maria Alieva[1,3,4,10], Lianne M. Wellens[1,3,4,10], Hendrikus C. R. Ariese[1,3,4], Paul R. Jamieson[5], Annelotte M. Vonk[6,7], Gimano D. Amatngalim[6,7], Huili Hu[2,3,4], Koen C. Oost[3,8], Hugo J. G. Snippert[3,8], Jeffrey M. Beekman[6,7], Ellen J. Wehrens[1,3,4], Jane E. Visvader[5,9,11], Hans Clevers[1,2,3,4,11] and Anne C. Rios[1,3,4,11]*

In vitro 3D organoid systems have revolutionized the modeling of organ development and diseases in a dish. Fluorescence microscopy has contributed to the characterization of the cellular composition of organoids and demonstrated organoids' phenotypic resemblance to their original tissues. Here, we provide a detailed protocol for performing high-resolution 3D imaging of entire organoids harboring fluorescence reporters and upon immunolabeling. This method is applicable to a wide range of organoids of differing origins and of various sizes and shapes. We have successfully used it on human airway, colon, kidney, liver and breast tumor organoids, as well as on mouse mammary gland organoids. It includes a simple clearing method utilizing a homemade fructose–glycerol clearing agent that captures 3D organoids in full and enables marker quantification on a cell-by-cell basis. Sample preparation has been optimized for 3D imaging by confocal, super-resolution confocal, multiphoton and light-sheet microscopy. From organoid harvest to image analysis, the protocol takes 3 d.

Introduction

The development of advanced culture methods has enabled the scientific research community to culture 'organs in a dish'[1]. These organoid systems self-organize into 3D structures and recapitulate phenotypic and functional traits of the original biological specimens. Organoid models have become instrumental in unraveling fundamental biological questions[2], modeling diseases such as cancer[3], and developing personalized treatment strategies[4–7]. Since the generation of the first intestinal organoid model[8], protocols have been extended to a wide range of healthy and cancerous tissues derived from organs such as prostate[9], brain[10], liver[11,12], stomach[13], breast[14,15], endometrium[16], salivary gland[17] and taste bud[18].

The development of organoids has coincided with the rise of novel volume imaging methods that can characterize the architecture of whole-mount tissues in 3D[19–22]; these represent a powerful imaging approach for probing the cellular complexity modeled with organoids[23]. Compared to traditional tissue-sectioning 2D imaging, 3D imaging is superior in visualizing the complexity of biological specimens. The superior qualities of 3D imaging are essential to understanding cellular composition, cell shape, cell-fate decisions and cell–cell interactions of intact biological samples. Non-invasive optical sectioning microscopic methods such as confocal or multiphoton laser scanning microscopy and, more recently, light-sheet fluorescence microscopy (LSFM), now make it possible to visualize fine cellular details as well as overall tissue architecture within a single biological sample. With the development of an increasing number of organoid systems and applications, 3D characterization of intact organoids at a single-cell level is highly valuable for demonstrating that they

[1]Princess Máxima Center for Pediatric Oncology, Utrecht, the Netherlands. [2]Hubrecht Institute, Royal Netherlands Academy of Arts and Sciences (KNAW) and University Medical Center (UMC) Utrecht, Utrecht, the Netherlands. [3]Department of Cancer Research, Oncode Institute, Hubrecht Institute-KNAW Utrecht, Utrecht, the Netherlands. [4]Cancer Genomics Center (CGC), Utrecht, the Netherlands. [5]Stem Cells and Cancer Division, The Walter and Eliza Hall Institute of Medical Research, Parkville, VIC, Australia. [6]Regenerative Medicine Center Utrecht, University Medical Center, Utrecht University, Utrecht, the Netherlands. [7]Department of Pediatric Pulmonology, Wilhelmina Children's Hospital, University Medical Center, Utrecht University, Utrecht, the Netherlands. [8]Molecular Cancer Research, Center for Molecular Medicine, University Medical Center Utrecht, Utrecht University, Utrecht, the Netherlands. [9]Department of Medical Biology, The University of Melbourne, Parkville, VIC, Australia. [10]These authors contributed equally: Maria Alieva, Lianne M. Wellens. [11]These authors jointly supervised this work: Jane E. Visvader, Hans Clevers, Anne C. Rios. *e-mail: a.c.rios@prinsesmaximacentrum.nl

reflect their in vivo counterparts and for analyzing mechanisms underlying cell lineage decisions and differentiation.

Here, we provide a detailed protocol for high resolution 3D imaging of entire organoids. This method is applicable to a wide range of organoids of differing origins and of various sizes, shapes and cellular content. We have recently used this method to reveal the morphology and cellular composition of newly developed organoid systems derived from various tissues, including airways[24], kidney[25], liver[11] and human breast cancer organoids[15]. Together with a multicolor fluorescent lineage–tracing strategy, this methodology has been used to reveal the bipotency of basal cells in mouse mammary organoids[14]. A graphical overview of the protocol is provided in Fig. 1a. In short, organoids are recovered from their 3D matrix, fixed and immunolabeled, optically cleared, and then 3D rendered with visualization software after imaging. The advantages of this method include the following:

- This protocol is widely applicable to a broad range of organoids, which vary in size, origin and morphology (Fig. 1b).
- This method allows imaging of entire immunolabeled organoids in 3D (Fig. 1c).
- Maintenance of native fluorescence is important for imaging organoids containing fluorescent reporter genes. This method allows for imaging of cultures that express reporter fluorophores such as the confetti locus proteins (Fig. 1d). Immunolabeling and fluorescent reporter visualization can be combined.
- This protocol includes a simple and non-toxic optical clearing step that allows imaging of complete (large) organoids with minimal light scattering.
- The protocol describes sample preparation for confocal, super-resolution confocal, multiphoton and light-sheet technology for faster imaging (Supplementary Video 1 and Fig. 2).
- Samples can be stored long term (for at least 6 months) with minimal loss of fluorescence.

Comparison with other methods

Other sample preparation methods have been developed for 3D imaging of intact biological samples (immunolabeling and optical clearing)[26]. However, clearing methodologies, including DISCO[27,28], CUBIC[29–31] and CLARITY[32,33], are often laborious protocols (requiring a few weeks of sample preparation with several steps and buffers) that were developed for very large tissues or organs. By contrast, this protocol (3 d) is designed and optimized for the handling of small and fragile organoid structures. Moreover, in contrast to other clearing methods, we provide a single-step non-toxic clearing agent that is both easy to make and safe to handle on a daily basis. As compared with 2D imaging techniques, the combination of (i) overnight incubation of antibodies for proper penetration to provide uniform staining throughout the organoid, (ii) an optical clearing step, (iii) microscopy scanning in the *x*, *y* and *z* directions (usually with multiple tiles) to capture complete organoids and (iv) processing of large 3D datasets requires investment of more time. In addition, although the procedure can be performed with commonly used laboratory reagents and equipment (a basic confocal microscope is sufficient), expensive licenses are required for optimal 3D rendering software, such as Imaris. However, free options such as Fiji can be explored.

Experimental design

Organoid harvesting (Steps 1–6)

Organoid cultures are often propagated in vitro by using matrices that mimic the in vivo extracellular environment and support their 3D structure. For most efficient antibody penetration during immunolabeling, the organoids are first extracted from Matrigel in a manner that maintains morphology. Efficient removal is influenced by the type of matrix, the number and size of organoids per drop and the time in culture after passaging, and requires optimization for different culture conditions. We have determined that for the types of organoids imaged here, which were grown in basement membrane extract (BME) or Matrigel, typically a 30- to 60-min step in ice-cold recovery solution is sufficient to dissolve matrices without damaging organoids.

Fixation (Steps 7–9)

Tissue fixation is a critical step in preserving tissue architecture and protein antigenicity, as well as minimizing autofluorescence. A 45-min fixation step with 4% (wt/vol) paraformaldehyde (PFA) at 4 °C is suitable for immunostaining a wide range of organoids (various sizes, shapes and origins). In general, longer fixation times (up to 4 h) are better suited to preserving fluorescence of reporters

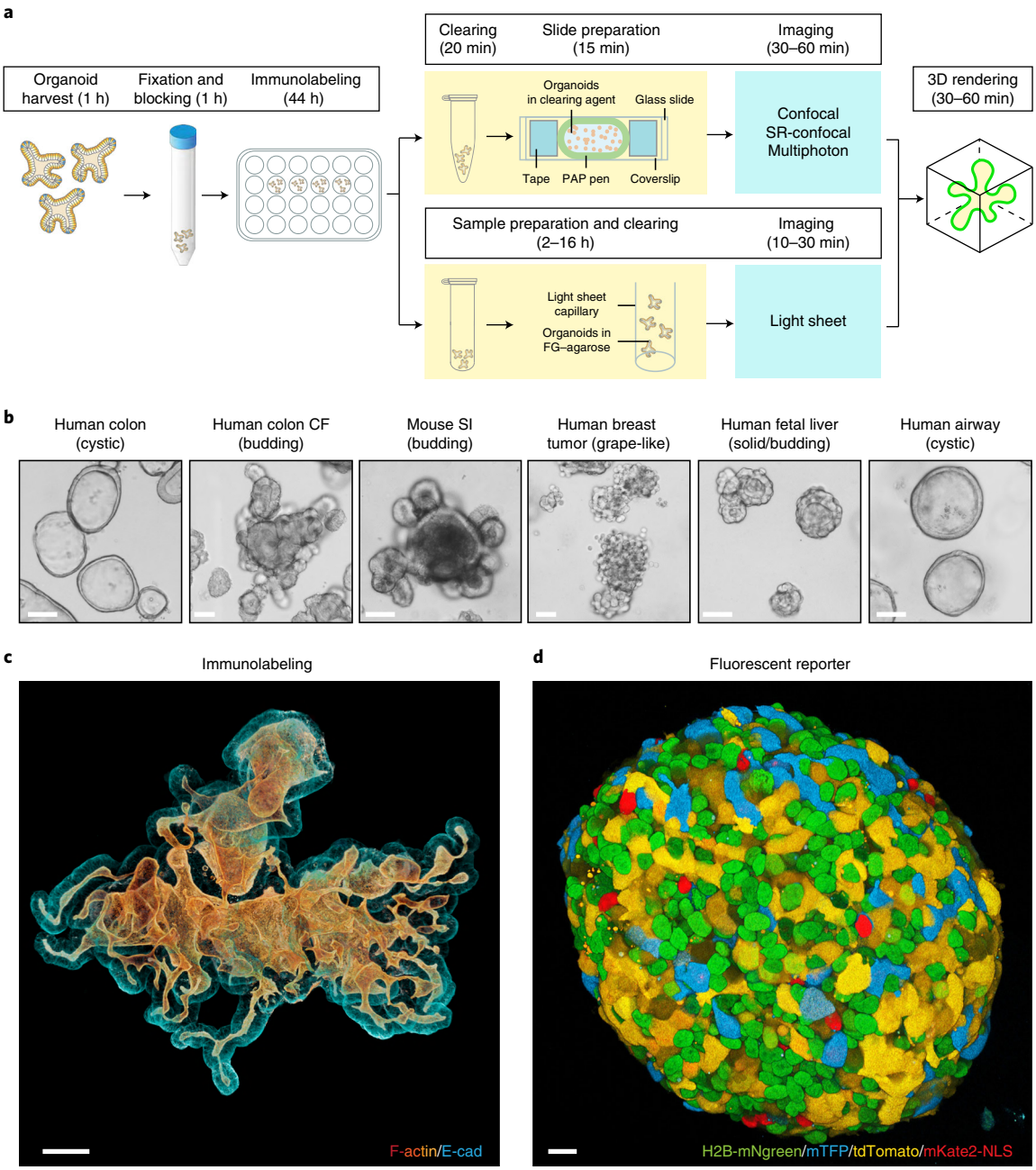

Fig. 1 | Overview of the high-resolution 3D imaging protocol. a, Schematic overview of the procedure. Organoids are recovered from their 3D matrix, and fixation and blocking are performed before immunolabeling with antibodies. An optical clearing step using a homemade fructose–glycerol (FG) clearing agent is performed to equalize the refractive index of the organoids and to reduce light scattering during imaging. Organoids can be imaged using single-photon confocal, super resolution (SR)-confocal, multiphoton or light-sheet microscopy. 3D rendering of images is performed using Imaris imaging software. **b**, Bright-field imaging of organoids of different origins representing the variation in organoid size and morphology between different organoid types that can be imaged in 3D using this sample preparation protocol. It includes human colon, human colon derived from a patient with cystic fibrosis (CF), mouse small intestine (SI), human breast tumor, human fetal liver and human airway organoids. Scale bars, 50 µm. **c**, Whole-mount 3D confocal image of a human colonic organoid immunolabeled for F-actin (red–yellow) and E-cadherin (E-cad; blue) (fructose–glycerol clearing; 25× oil objective). Scale bar, 40 µm. **d**, Whole-mount 3D confocal image of a human breast tumor organoid that expresses a confetti construct containing the fluorescent proteins H2B-mNeon green (H2B-mNgreen; green), mTFP (blue), tdTomato (yellow) and mKate2-NLS (red) (fructose–glycerol clearing; 40× oil objective). Scale bar, 10 µm. **c** and **d** were rendered in Imaris using the 'blend 3D' mode.

expressed in organoids, such as the confetti reporter proteins (H2B-mNeongreen, mTFP, tdTomato and mKate2-NLS, which were adapted from Snippert et al.[34]; Fig. 1d). For cystic organoids, we sometimes observe collapsing structures during fixation. For these particular cases, alternative fixative methods, including formalin or PFA–glutaraldehyde (2% (vol/vol)) can be used; these help preserve

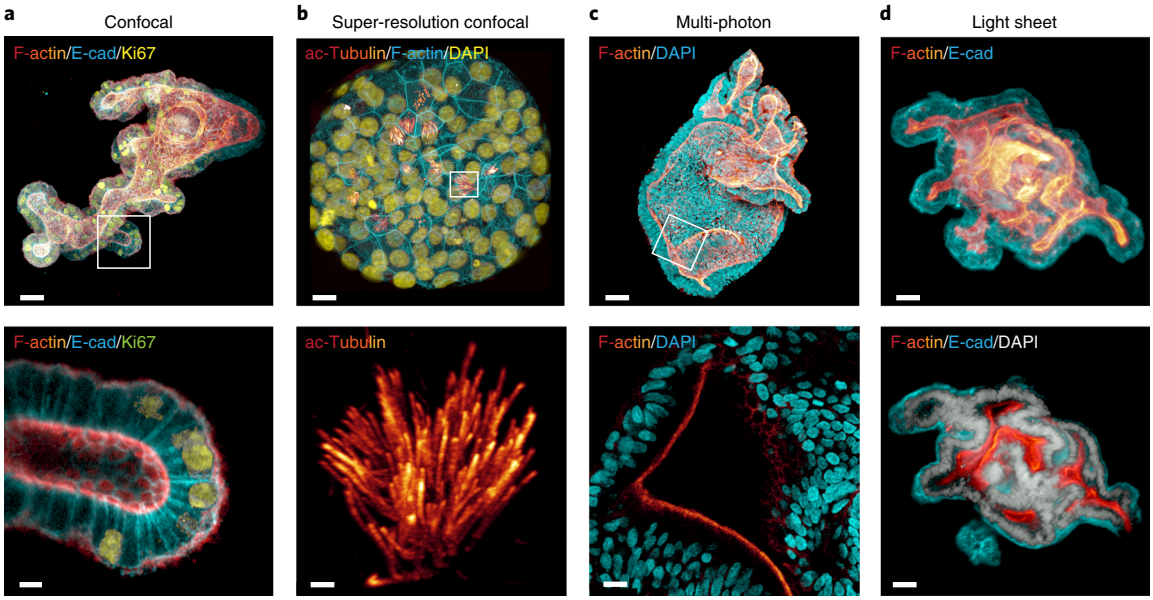

Fig. 2 | Representative 3D whole-mount organoid images obtained with different light microscopy technologies. a, Whole-mount 3D confocal image (top) and enlarged optical section (bottom) of a human colonic organoid immunolabeled for F-actin (red–yellow), E-cadherin (E-cad; blue) and Ki67 (yellow) (fructose–glycerol clearing; 25× oil objective). Scale bars, 20 µm (top) and 5 µm (bottom). **b**, The Airyscan Fast module was used to obtain a confocal 3D whole-mount image (top) and enlarged area (bottom) of a human airway organoid immunolabeled with acetylated-tubulin (ac-Tubulin; red–yellow), F-actin (blue) and DAPI (yellow) (40× water objective). Scale bars, 15 µm (top) and 2 µm (bottom). **c**, Multiphoton 3D whole-mount image (top) and enlarged optical section (bottom) of a human colonic organoid labeled for F-actin (red–yellow) and DAPI (blue) (no clearing; 32× water objective). Scale bars, 50 µm (top) and 10 µm (bottom). **d**, Light-sheet 3D whole-mount image (top) and optical section (bottom) of a human colonic organoid immunolabeled for F-actin (red–yellow), E-cadherin (E-cad; blue) and DAPI (white) (fructose–glycerol clearing; 20× objective). Scale bars, 15 µm. **a**–**c** were rendered in Imaris using the transparent 3D mode (MIP mode), and **d** was rendered in Imaris using the blend 3D mode.

fragile tissue architecture. However, these two methodologies can impair fluorescent reporter detection and increase background autofluorescence.

Immunolabeling (Steps 12–23)

Organoids may consist of a polarized epithelial monolayer, in which the apical membrane lines a central lumen, or may present as more solid multilayered epithelial structures, which is the case for most tumor-originated cultures (Fig. 1b). Organoids can reach large sizes, and appropriate antibody incubation times are important for proper penetration. It is important to wash the samples extensively to avoid background or loss of signal.

Clearing (Step 24)

High scattering of thick tissues can be a hurdle for the optical imaging of 3D structures because of the mismatching of refractive indices between different cellular components. Over the past few years, there have been significant advances in overcoming this scattering through tissue-clearing techniques (e.g., the DISCO[27,28], CUBIC[29–31] and CLARITY[32,33] protocols). However, these clearing methodologies may be too harsh for fragile tissues such as organoids. We provide a simple, non-toxic optical clearing step that facilitates imaging of complete organoids, thereby limiting the decline in fluorescence in the *z* direction (Fig. 3a). It is applicable to either immunolabeled organoids (Fig. 1c) or fluorescent reporter detection (Fig. 1d) and is suitable for most light microscopy technologies (Fig. 2). By comparing different clearing reagents, we observed that both commercially available FocusClear and our homemade fructose–glycerol clearing agent were able to efficiently clear the tissue and thus limit the decrease in fluorescence intensity in the *z* direction (Fig. 3b). However, immersion of organoids in FocusClear led to an overall fluorescence quenching and loss of signal intensity (Fig. 3c). Optical clearing is important to obtaining a cellular resolution suitable for performing automated cellular segmentation and quantification algorithms. Importantly, immunolabeled organoids can be stored long term (up to 6 months) in the fructose–glycerol-based clearing solution at −20°C. In addition, the clearing step is reversible, and new antibodies can be added to initial stainings with no loss of resolution or brightness.

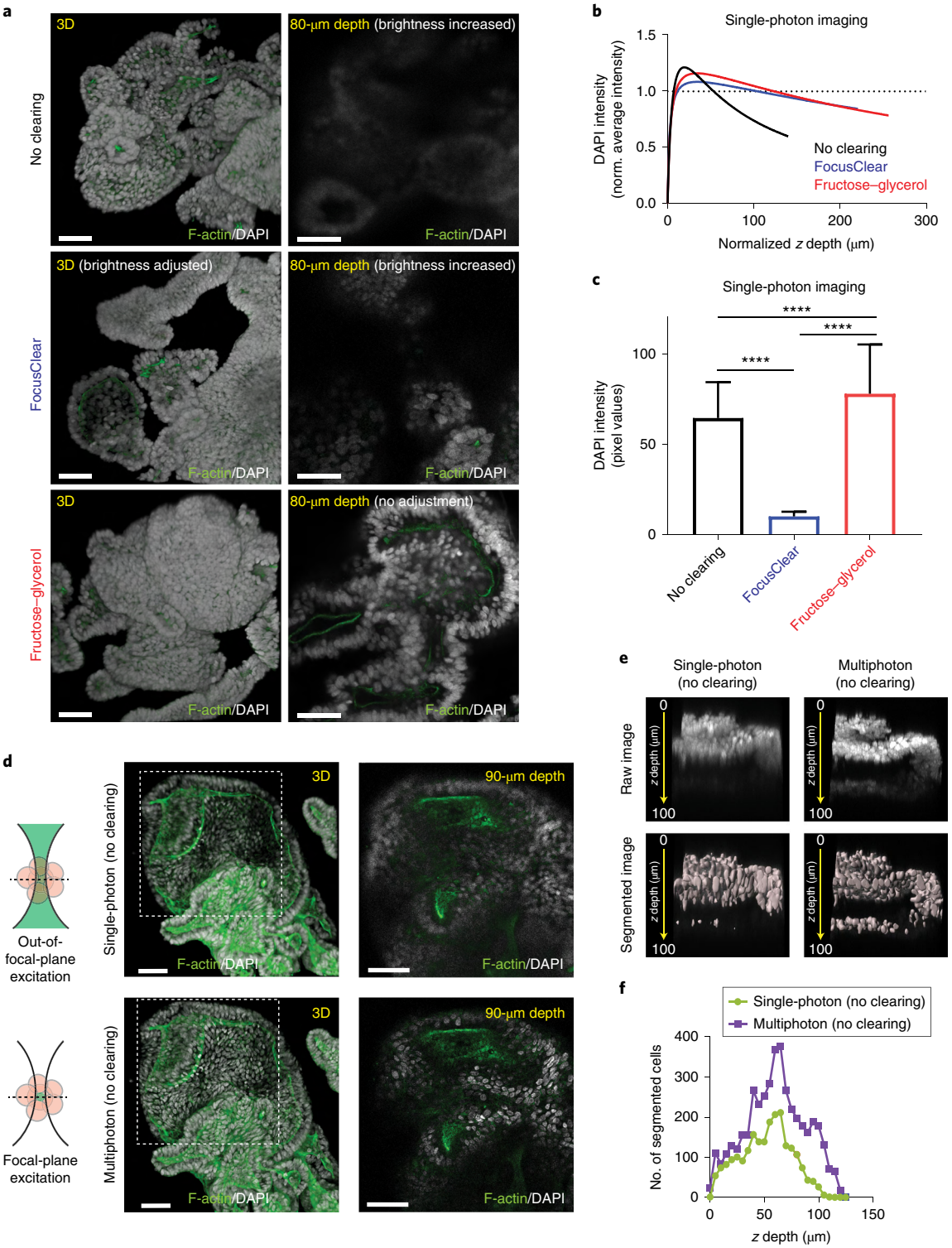

Slide preparation and storage (Step 24)

In contrast to imaging monolayers of adherent cells, mounting of 3D organoids requires a refined method for slide preparation. We use double-sided sticky tape to lift the coverslip, thereby maintaining 3D organoid morphology (and fixing the coverslip to the slide). The viscous clearing agent we use in our protocol is optimal for keeping organoids in place during slide preparation and while imaging. It is advised that organoids be imaged directly after mounting for optimal detection.

◀ **Fig. 3 | Comparison of different optical clearing agents and single- and multiphoton imaging. a–e**, Human colonic organoids were stained with F-actin (green) and DAPI (gray) and imaged with single-photon (**a–c**) or both single-photon and multiphoton (**d**,**e**) microscopy. **a**, Representative images of human colonic organoids imaged without clearing, or cleared with FocusClear or fructose–glycerol (25× water objective). (Left) 3D reconstruction of the organoid. (Right) cross-section of the organoid at an 80-μm depth. Note that, for the 'No clearing' and 'FocusClear' conditions, the brightness of the image was increased as compared to that of the 'Fructose–glycerol' condition to visualize the organoid. Scale bars, 50 μm. **b**, Non-linear regression fit analyzed in GraphPad Prism 6 between DAPI intensity and *z* depth for different clearing methods. For each imaged organoid, the DAPI intensity was normalized to the average intensity of all the organoids. Values represent intensities of individual cells detected by DAPI segmentation and analyzed by the v.8.2.1 Imaris software. **c**, Bar graph plotted in GraphPad Prism 6 showing average DAPI intensity with different clearing methods. Data depicted as mean ± s.d. Values are intensities of >4,000 individual cells detected by DAPI segmentation. $^{****}P < 0.0001$, Kruskal–Wallis test with two-sided Dunn's multiple comparison post hoc testing. **d**, Representative images of the same colonic organoid imaged with single-photon (top) or multiphoton (bottom) microscopy (no clearing; 20× dry objective). (Left) 3D reconstruction of the organoid. (Right) Cross-section of the organoid at a 90-μm depth; images correspond to the dashed boxes in the images on the left. Scale bars, 50 μm. **e**, Representative raw images (top) and DAPI-segmented images (bottom) of the same cystic fibrosis organoid imaged with single-photon or multiphoton microscopy. Loss of resolution in *z* is delimited by the decrease in the number of cells that can be detected. Image segmentation was achieved using local contrast of the nuclear staining intensity with the Imaris software. Touching objects were split on the basis of a minimal distance of 4 μm. Finally, surfaces with a voxel size >10 were selected. **f**, Histogram plotted in GraphPad Prism 6 showing the number of segmented cells per *z* cross-section of the same organoid imaged with single-photon or multiphoton microscopy. Images in **a** and **d** were rendered in Imaris using the transparent 3D mode (MIP mode).

However, once mounted, slides can be stored at 4 °C for at least 1 week and at −20 °C for at least 6 months following fructose–glycerol-based clearing. For light-sheet imaging, a modified clearing solution containing low-melting-point (LMP) agarose is used to hold the sample.

Microscopy (Step 25)

Imaging and visualization modalities applicable to complex structures include single-photon confocal, multiphoton and LSFM. Each system has specific features and applications based on compromises between the imaging speed, resolution and convenience of use. Confocal (single-photon) microscopy provides high-quality imaging with high single-cell resolution but with an accompanying rapid decrease in intensity with increasing depth, whereas multiphoton microscopy enables deep imaging into tissues. Optical clearing is not advised for cystic organoids containing large lumens (see 'Troubleshooting' section for Step 24A(iii)). For these types of organoids, we advise multiphoton imaging without clearing. To support this, we show that multiphoton imaging is superior to single-photon imaging of organoids that were not optically cleared (Fig. 3d–f). Furthermore, multiphoton excitation provides higher 3D resolution of large organoids, as fluorophores are excited in only one focal plane (Fig. 3d). To illustrate this, we performed nuclear segmentation of the same organoid imaged using single-photon and multiphoton microscopy (Fig. 3d). Although the two imaging methods gave similar nuclear resolution on the surface of the organoid, multiphoton microscopy performed better at deeper layers (Fig. 3d–f). As both techniques use point-by-point scanning along the entire sample, imaging is relatively time consuming and may lead to bleaching of fluorophores (photobleaching)[35]. Yet we rarely observed loss of intensity due to photobleaching. By contrast, LSFM provides fast optical sectioning with minimal photobleaching of large tissue samples. However, it requires the imaging specimen to be completely cleared, and obstacles such as air bubbles can cause shadows along the illumination path[36]. In addition, the resolution obtained with light-sheet imaging remains suboptimal, as compared with confocal and multiphoton microscopy, for obtaining sub-cellular resolution (Fig. 2d).

Materials

Biological materials

- Organoids of human or murine origin. We have successfully used mouse small intestinal organoids, human colonic organoids, human breast tumor organoids, human fetal liver organoids, human airway organoids and murine mammary gland organoids. Mammary gland organoids can be derived from 6- to 10-week-old wild-type FVB/N female mice (obtained from the Walter and Eliza Hall Institute (WEHI) Animal Facility). **! CAUTION** Use of animals or human material for research purposes requires approval from institutional and national regulatory bodies. Do not proceed without appropriate approval and, for materials derived from human tissues, informed consent from all

subjects. All our animal experiments conformed to regulatory standards and were approved by the Walter and Eliza Hall Institute (WEHI) Animal Ethics Committee. All human organoid samples were obtained from biobanks through Hubrecht Organoid Technology (HUB, www.hub4organoids.nl). Authorizations were obtained from the medical ethical committee of UMC Utrecht (METC UMCU) at the request of HUB in order to ensure compliance with the Dutch Medical Research Involving Human Subjects Act, and informed consent was obtained from donors when appropriate.

Reagents

- Paraformaldehyde (PFA) powder (Sigma-Aldrich, cat. no. P6148-500g) **! CAUTION** PFA is hazardous. Manipulate in a fume hood. Avoid direct contact with skin. Wear rubber gloves and protective eye goggles.
- Sodium hydroxide (NaOH) pellets (10 M stock solution; Merck Millipore, cat. no. 567530) **! CAUTION** NaOH is corrosive. Wear rubber gloves and protective eye goggles.
- Hydrochloric acid (HCl; 10 M stock solution; Ajax FineChem, cat. no. 256.2.5L-PL) **! CAUTION** HCl is corrosive. Manipulate in a fume hood. Wear rubber gloves and protective eye goggles.
- BSA (Sigma-Aldrich, cat. no. A3059)
- Tween 20 (Sigma-Aldrich, cat. no. P7949)
- Triton X100 (Sigma-Aldrich, cat. no. T8532) **! CAUTION** Triton X100 is hazardous. Avoid contact with skin and eyes.
- PBS (Dulbecco's phosphate-buffered saline, 1×; Gibco, cat. no. 14190144)
- Fructose (Sigma-Aldrich, cat. no. F0127)
- Glycerol (Ajax FineChem, cat. no. 242-500ml)
- Cell recovery solution (Corning, cat. no. 354253)
- FocusClear (CelExplorer, cat. no. FC-101)
- UltraPure low-melting-point (LMP) Agarose (Thermo Fisher, cat. no. 16520050)
- Primary antibodies, user specific (see Table 1 for details of antibodies that we used successfully in human and mouse organoid tissues)
- Secondary antibodies: unconjugated primary antibodies are labeled with species-specific secondary antibodies containing the desired fluorophore (e.g., Donkey Anti-Mouse IgG (H+L) Highly Cross-Adsorbed Alexa Fluor 488, Life Technologies, cat. no. A-21202)
- DAPI (stock solution, 1 mg/ml, 1:500 dilution; Thermo Fisher, cat. no. D9542)
- Alexa Fluor 647 phalloidin (1:100 dilution, for staining F-actin; Thermo Fisher, cat. no. A22287)
- SDS (sodium dodecyl sulfate; Sigma-Aldrich, cat. no. L6026)

Equipment

Organoid harvesting

- Conical tubes (15 ml; Greiner BioOne, cat. no. 5618-8271)

Immunostaining

- Conical tubes (15 ml; Greiner BioOne, cat. no. 5618-8271)
- 2-ml Safe-lock centrifuge tubes (Eppendorf, cat. no. EP0030 120.094)
- Suspension cell culture plates (24-well; Greiner Bio-One, cat. no. 662102)
- Horizontal shaker (VWR, cat. no. 444-2900)
- Magnetic stirrer (IKA, cat. no. 0005019700)

Slide preparation for confocal and multiphoton microscopy

- 1.5-ml Safe-lock centrifuge tubes (Eppendorf, cat. no. EP0030 120.094)
- Dissection stereomicroscope (Leica, model no. M205 FA)
- Cover glass, no. 1.5 (24 × 60 mm; VWR, cat. no. 630-2108)
- Cover glass, no. 1.5 (48 × 60 mm; ProSciTech, cat. no. G425-4860)
- Microscope slides (Superfrost, ground edge, 90°, 26 × 76 mm; Menzel Gläser; Thermo Fisher, cat. no. AA00008032E00MNT10)
- Ace O-rings (fluoroelastomer with tetrafluorolethylene additives (FETFE), 23.5 mm, wall size 1.78 mm; Sigma-Aldrich, cat. no. Z504785)
- Graduated transfer pipettes (small bulb; Samco, cat. no. 222-15)
- Double-sided sticky tape (12.7 mm × 6.35 m; Scotch 3M)

Table 1 | List of successfully tested antibodies for 3D imaging

Antigen	Clone	Conjugate	Species	Supplier	Catalog number	Organoid origin	Dilution
K14	Polyclonal	Unconjugated	Rabbit	Thermo Fisher Scientific	PA5-28002	Mouse breast	1:500
K5	Polyclonal Poly19055	Unconjugated	Rabbit	BioLegend (formerly Covance)	905501	Mouse breast	1:500
K8/18	(TROMA-I)	Unconjugated	Rat	DSHB (University of Iowa)	N/A	Mouse breast	1:200
p63	4A4	Unconjugated	Mouse	Abcam	ab735	Mouse breast	1:200
E-cadherin	E-CCD2	Unconjugated	Rat	Thermo Fisher Scientific	13-1900	Mouse breast	1:400
ERα	MC-20 polyclonal	Unconjugated	Rabbit	Santa Cruz Biotechnology	sc-542	Mouse breast	1:200
Milk	Polyclonal	Unconjugated	Rabbit	Accurate Chemical & Scientific Corporation	YNRMTM	Mouse breast	1:500
Her2	SP3	Unconjugated	Rabbit	Thermo Fisher Scientific	RM-9103-S1	Human breast tumor	1:400
K7	OV-TL 12/30	Unconjugated	Mouse	Thermo Fisher Scientific	MA5-11986	Human liver	1:200
K19	D7F7W	Unconjugated	Rabbit	Cell Signaling Technology	13092S	Human liver	1:200
EpCam	G8.8	Allophycocyanin	Rat	Thermo Fisher Scientific	17-5791-80	Human liver	1:200
MRP2	M2 III-6	Unconjugated	Mouse	Abcam	ab3373	Human liver	1:50
E-cadherin	36/E-Cadherin	Unconjugated	Mouse	BD Biosciences	610182	Various human	1:400
K5	Polyclonal	Unconjugated	Rabbit	BioLegend (formerly Covance)	905501	Human airway and breast	1:800
Acetylated-tubulin	6-11 B-1	Unconjugated	Mouse	Santa Cruz Biotechnology	sc-23950	Human airway	1:100
CC-10	S-20	Unconjugated	Goat	Santa Cruz Biotechnology	sc-9773	Human airway	1:100
MUC5ac	EPR16904	Unconjugated	Rabbit	Abcam	ab198294	Human airway	1:400
F-actin (phalloidin)	N/A	Alexa Fluor 555/ 647	N/A	Thermo Fisher Scientific	A34055/ A22287	Various, mouse and human	1:100
DAPI	N/A	Unconjugated	N/A	Thermo Fisher Scientific	P36935	Various, mouse and human	1:400
Rat-IgG	N/A	Biotin	Rabbit	Vector Laboratories	BA-4001	Various, mouse and human	1:200
Streptavidin (recognizes biotinylated antibodies)	N/A	Pacific Blue	N/A	Thermo Fisher Scientific	S-11222	All origins	1:300
GFP	Polyclonal	Unconjugated	Chicken	Abcam	ab13970	Various, mouse and human	1:250
ZO-1	Polyclonal	Unconjugated	Rabbit	Thermo Fisher Scientific	40-2200	Human kidney	1:100
Integrin	MP 4F10	Unconjugated	Mouse	Abcam	ab20142	Human kidney	1:200
Claudin	Polyclonal	Unconjugated	Rabbit	Abcam	ab15102	Human kidney	1:200
Villin	1D2C3	Unconjugated	Mouse	Santa Cruz Biotechnology	sc-58897	Human kidney	1:200
Acetylated tubulin	6-11 B-1	Unconjugated	Mouse	Santa Cruz Biotechnology	sc-23950	Human kidney	1:200
Keratine	Polyclonal	Unconjugated	Rabbit	Dako	Z0622	Human kidney	1:200
β-catenin	H-102	Unconjugated	Rabbit	Santa Cruz Biotechnology	sc-7199	Human kidney	1:200
E-cadherin	36/E-cadherin	Unconjugated	Mouse	BD Biosciences	610182	Human kidney	1:250
GATA3	HG3-31	Unconjugated	Mouse	Santa Cruz Biotechnology	sc-268	Human kidney	1:50
AQP3	Polyclonal	Unconjugated	Rabbit	Abcam	ab125219	Human kidney	1:200
AE1	Polyclonal	Unconjugated	Rabbit	Alpha Diagnostic International	AE11-A	Human kidney	1:250
Rabbit IgG (H+L)	Polyclonal	Alexa Fluor 488	Donkey	Thermo Fisher Scientific	A-21206	All samples	1:500
Rabbit IgG (H+L)	Polyclonal	Alexa Fluor 555	Donkey	Thermo Fisher Scientific	A-31572	All samples	1:500
Rabbit IgG (H+L)	Polyclonal	Alexa Fluor 647	Donkey	Thermo Fisher Scientific	A-31573	All samples	1:500
Mouse IgG (H+L)	Polyclonal	Alexa Fluor 488	Donkey	Thermo Fisher Scientific	A-21202	All samples	1:500
Mouse IgG (H+L)	Polyclonal	Alexa Fluor 555	Donkey	Thermo Fisher Scientific	A-31570	All samples	1:500
Mouse IgG (H+L)	Polyclonal	Alexa Fluor 647	Donkey	Thermo Fisher Scientific	A-31571	All samples	1:500
Goat IgG (H+L)	Polyclonal	Alexa Fluor 488	Donkey	Thermo Fisher Scientific	A-11055	All samples	1:500
Goat IgG (H+L)	Polyclonal	Alexa Fluor 555	Donkey	Thermo Fisher Scientific	A-21432	All samples	1:500
Goat IgG (H+L)	Polyclonal	Alexa Fluor 647	Donkey	Thermo Fisher Scientific	A-21447	All samples	1:500
Rat IgG (H+L)	Polyclonal	Alexa Fluor 488	Donkey	Thermo Fisher Scientific	A-21208	All samples	1:500
Rat IgG (H+L)	Polyclonal	Alexa Fluor 555	Goat	Thermo Fisher Scientific	A-21434	All samples	1:500
Rat IgG (H+L)	Polyclonal	Alexa Fluor 647	Goat	Thermo Fisher Scientific	A-21247	All samples	1:500
Chicken IgY (H+L)	Polyclonal	Alexa Fluor 488	Goat	Thermo Fisher Scientific	A-11039	All samples	1:500

DSHB, Developmental Studies Hybridoma Bank; H+L, heavy and light chains; N/A, not available.

• PAP pen (DAKO, cat. no. S2002) ▲ CRITICAL Pens from different brands vary in their capacity to prevent the fructose–glycerol clearing agent from spreading out over the coverslip.

Sample preparation for light-sheet microscopy
• Capillary (size ~1.5 mm; Carl Zeiss Microscopy, cat. no. 701908) with associated plunger (Carl Zeiss Microscopy, cat. no. 701998)

Microscopy platforms and objectives
• Confocal microscopes (Zeiss, model no. LSM 880 (25×, numerical aperture (NA) 0.8, multi-immersion; 32× NA 0.85, water immersion; and 40× NA 1.3, oil immersion; working distance: 570 µm, 1.1 mm and 210 µm, respectively)
• Multiphoton microscope (Zeiss, model no. LSM 880 (32×, NA 0.85, water immersion, working distance: 1,100 µm)
• Light-sheet microscope: Zeiss Light Sheet . (illumination objective: 10×, NA 0.2; detection objective: 20×, clearing immersion, NA 1.0, $n = 1.45 \pm 0.03$, working distance: 5.6 mm)

Image processing
• Dell Precision workstation (64-bit, Windows 8, 512 GB RAM, AMD Radeon R9 200 series graphics card)

Software
• Imaris v.8.2.1 for 3D and 3D stereo visualization and segmentation of confocal and multiphoton data (Bitplane, http://www.bitplane.com/imaris)
• Arivis tiling and 3D reconstruction software for light-sheet datasets (Vision 4D, https://www.arivis.com/)
• ZEN Black software (the link for downloading the software is available upon request through the Zeiss website (https://www.zeiss.com/microscopy/int/products/microscope-software/zen.html)
• GraphPad Prism 6 (https://www.graphpad.com/scientific-software/prism/)

Reagent setup

PFA (4% (wt/vol))
To prepare 4% (wt/vol) PFA, heat 500 ml of PBS to 60 °C in a microwave. Add 20 g of PFA and dissolve on a stirrer. Add a few drops of 10 M NaOH. Cool on ice and adjust the pH to 7.4 by adding a few drops of 10 M HCl (store at −20 °C for up to 2 months).

PBT (0.1% (vol/vol))
To prepare 0.1% (vol/vol) PBS-Tween (PBT), add 1 ml of Tween 20 to 1,000 ml of PBS (store at 4 °C for up to 4 weeks).

Organoid washing buffer
To prepare organoid washing buffer (OWB), add 1 ml of Triton X-100 and 2 g of BSA to 1 liter of PBS (store at 4 °C for up to 2 weeks).

Fructose–glycerol clearing solution
Fructose–glycerol clearing solution is 60% (vol/vol) glycerol and 2.5 M fructose. To prepare 660 ml of this solution, mix 330 ml of glycerol, 70 ml of dH_2O and 297.2 g of fructose on a magnetic stirrer. Refractive index = 1.4688 at room temperature (RT: 19–23 °C). Store at 4 °C in dark for up to 1 month.

PBS–BSA (1% (wt/vol))
To prepare 1% (wt/vol) PBS–BSA, dissolve 1 g of BSA in 100 ml of PBS (store at 4 °C for up to 2 weeks)

Light-sheet embedding solution
To prepare light-sheet embedding solution, dissolve 0.4 g of LMP agarose in 10 ml of water using a microwave and let it cool to 40 °C on a heat block with a magnetic stirrer. Add 10 ml of fructose–glycerol clearing solution (40 °C) and mix on a heat block with a magnetic stirrer until the solution is clear; keep at 40 °C until use. ▲ CRITICAL Prepare the solution fresh every time.

Procedure

Organoid recovery from 3D matrix ● Timing 1–1.5 h

▲ CRITICAL This section describes recovery of organoid cultures grown in drops of BME or Matrigel from a 24-well plate. We recommend using organoids with a size ranging from 100 to 500 µm and to use one confluent culture well per staining. Depending on the organoid size and origin, the well should ideally contain 50–200 organoids for confocal or multiphoton imaging and 100–200 organoids for light-sheet imaging.

1 Remove the culture medium from the wells and wash with 1 ml of PBS without disrupting the 3D matrix.

2 Put the plate on ice, add 1 ml of ice-cold cell recovery solution to each well and incubate on a horizontal shaker at 4 °C (60 r.p.m.) for 30–60 min. After incubation, the 3D drops should be dissolved.

3 Precoat the inside and outside of a 1-ml tip with protein by dipping the full length of the tip in 1% (wt/vol) PBS–BSA and resuspending 1 ml of 1% (wt/vol) PBS–BSA two times. This will prevent the organoids from sticking to the tip. After coating the tip, gently resuspend the contents of the well five to ten times.

? TROUBLESHOOTING

4 Transfer the organoids to a 15-ml tube precoated with 1% (wt/vol) PBS–BSA. Pool organoids from different wells but with the same identity in the same tube.

5 Rinse out the culture well with 1 ml of ice-cold 1% (wt/vol) PBS–BSA to collect all organoids.

6 Fill up to 10 ml with cold PBS and spin down at 70*g* for 3 min at 4 °C. Remove the supernatant. The pellet should be tight without a visible layer of 3D matrix.

▲ CRITICAL STEP Organoid recovery from the 3D matrix is essential for optimal immunolabeling. Remaining 3D matrix can hamper proper antibody penetration of the organoid structure or lead to high background staining due to a specific binding of antibodies to the matrices.

Fixation and blocking ● Timing 1 h

7 Gently resuspend the pellet of organoids in 1 ml of PFA, using a 1-ml tip precoated with 1% (wt/vol) PBS–BSA as described in Step 3.

8 Incubate at 4 °C for 45 min (halfway through the incubation period, gently resuspend the organoids, using a 1-ml tip precoated with 1% (wt/vol) PBS–BSA). During fixation, a minimal change in morphology is observed for most mono- or multilayered organoids. However, fixation can cause spherical, monolayered organoids that contain large fluid-filled lumens to 'collapse'. This has been observed for human intestinal samples and may depend on the donor and the quality of the culture medium.

? TROUBLESHOOTING

9 Fill the tube up to 10 ml with cold (4 °C) PBT, gently mix by swirling the tube, incubate for 10 min at 4 °C and spin down at 70*g* for 5 min at 4 °C. From this step onward, precoating of tips is not needed.

■ PAUSE POINT Organoids can be stored in PBT at 4 °C for 2 d or over the weekend, but, ideally, one should continue with the next steps as soon as possible.

10 For blocking the organoids, resuspend the pellet in cold (4 °C) OWB and transfer the appropriate amount of organoids per staining to a low-adherence/suspension 24-well plate (use at least 200 µl per well).

▲ CRITICAL STEP Compared to blocking and immunolabeling in tubes or Eppendorf tubes, the 24-well format allows gentle movement of organoids for optimal antibody penetration and washings, and allows organoid visualization at any moment during the procedure using microscopy.

? TROUBLESHOOTING

11 Incubate at 4 °C for 15 min.

Immunolabeling ● Timing 44 h

12 Add 200 µl of OWB to one of the empty wells and use this as a reference well.

13 Make sure that the organoids are settled at the bottom of each well; then tilt the plate to 45° and remove the OWB, leaving the organoids in 200 µl of OWB (use the reference well to estimate 200 µl).

14 Add 200 µl of OWB with primary antibodies (2× concentration) to each well and incubate overnight at 4 °C with mild rocking/shaking (60 r.p.m. on a horizontal shaker).

15 Add 1 ml of OWB per well.
16 Wait for 3 min until all organoids are settled at the bottom of each well.
17 Remove 1 ml of OWB, leaving 200 µl in each well.
18 Add 1 ml of OWB per well and incubate for 2 h with mild rocking/shaking.
19 Repeat Steps 16–18 two more times.
20 Wait for 3 min, until all organoids are settled at the bottom of each well.
? TROUBLESHOOTING
21 Remove 1 ml of OWB, leaving 200 µl in each well.
22 Add 200 µl of OWB with secondary antibodies (2× concentration) per well and incubate overnight at 4 °C with mild rocking/shaking.
23 Repeat Steps 15–19. Transfer the organoids of each well to a 1.5-ml (confocal or multiphoton imaging) or 2-ml (light-sheet imaging) Eppendorf tube and let the organoids settle at the bottom or spin down (70*g*, 4 °C, 2 min).
▲ CRITICAL STEP Reagent changes and organoid transfers can cause sample loss during fixation and immunolabeling. A loss of ≤10–20% of the initial number of organoids in the culture well (Step 1) is expected. We advise reading 'Troubleshooting' section for Steps 1, 10 and 20 to ensure a minimal loss of sample.
■ PAUSE POINT At any point between Steps 12 and 23, the organoids can be stored in OWB (with or without antibodies) at 4 °C for 2 d or over the weekend without rocking, but, ideally, one should continue with the next steps as soon as possible.

Sample preparation for imaging

24 Continue with confocal or multiphoton sample preparation (option A) or with light-sheet sample preparation (option B).

(A) **Sample preparation for single-photon confocal or multiphoton imaging ● Timing 35 min**
(i) *Clearing*. Remove as much of the OWB as possible without touching the organoids.
(ii) Add fructose–glycerol clearing solution (minimum of 50 µl at RT) using a 200-µl tip with the end cut off and resuspend gently. Prevent bubble formation.
▲ CRITICAL STEP The fructose–glycerol clearing solution has high viscosity. It is therefore difficult to handle small volumes. Make sure to use the fructose–glycerol clearing solution at RT and pipette slowly and carefully.
(iii) Incubate at RT for 20 min. Clearing causes organoid shrinkage. This does not change the general morphology of most mono- and multilayered organoids, but it can alter the spherical shape of mono-layered organoids with large lumens.
? TROUBLESHOOTING
■ PAUSE POINT At this stage, the sample can be stored at 4 °C (for at least 1 week) or −20 °C (for at least 6 months).
(iv) *Slide preparation for imaging*. Draw a 1 × 2-cm rectangle in the middle of a slide, using a PAP pen.
(v) Place a 1-cm-long piece of sticky tape at both sides of the rectangle. Use 1, 2 or 3 layers, depending on the organoid size.
(vi) Cut off the end of a 200-µl tip and use it to place the organoids in the middle of the rectangle. Use 20 µl per layer of tape.
(vii) Place a coverslip on top. Place the left side of the coverslip on the left stack of sticky tape and then slowly lower the right side of the coverslip until it touches the right stack of sticky tape; then let go of the coverslip.
(viii) Wait for 1 min to allow the fluid to spread out.
(ix) Gently apply pressure to both sides of the coverslip to firmly attach it to the double-sided sticky tape. The slide is now ready for imaging.
■ PAUSE POINT At this stage, the sample can be stored at 4 °C (for at least 1 week) or −20 °C (for at least 6 months).

(B) **Sample preparation for light-sheet microscopy ● Timing 2–16 h**
(i) Remove most of the OWB and place the Eppendorf tube on a heat block at 40 °C.
(ii) Before the pellet dries out, resuspend the pellet in 300 µl of light-sheet embedding solution and put back at 40 °C.
(iii) While the Eppendorf tube is at 40 °C, use a light-sheet glass capillary to aspirate the mix and let it solidify at 4 °C.

(iv) Place the capillary containing the sample in the light-sheet chamber and fill the chamber with fructose–glycerol clearing solution.

(v) Push down the agarose-based clearing solution (light-sheet embedding solution) of the capillary to expose the sample for imaging.

▲ CRITICAL STEP The quality of light-sheet images is severely affected by the presence of air bubbles or other small objects in the light path, so work cleanly and prevent bubble formation. In addition, allow the sample to settle in the imaging chamber for a couple of hours to overnight at RT before imaging.

Imaging and image processing

25 Proceed with single-photon or multiphoton (option A) or light-sheet (option B) imaging.

(A) **Single-photon and multiphoton imaging** ● Timing **1–2 h**

(i) Use a confocal microscope to image the slide, using a multi-immersion 25× or oil immersion 40× objective for single-photon imaging or a 32× water immersion objective for multiphoton imaging. The acquisition mode settings we use most commonly are as follows: scan mode = frame, frame size = 1,024 × 1,024, line step = 2, bidirectional scanning, speed = 7, averaging number = 1, bit depth = 12 and bidirectional scanning. Activate the *z*-stack mode and define the lower and upper limits. For imaging large organoids or multiple organoids together, activate the tile scan and indicate the borders of the organoids. Of note, other confocal microscopes can be used for similar results (we have tested the protocol with the Leica SP8 and Olympus FV 3000).

? TROUBLESHOOTING

(ii) For tile scan acquisition, stitch the imaging using the ZEN Black software (Imaris, Fiji or ImageJ software can also be used).

? TROUBLESHOOTING

(iii) Use the 3D view tab in the Imaris imaging software to optimize brightness, contrast and 3D-rendering properties for the best representation of the imaging. After corrections, the RGB images can be exported as TIFF files.

(B) **Light-sheet imaging** ● Timing **40–90 min**

(i) Use a light-sheet microscope to image the samples in the light-sheet embedding solution, using a 20× detection objective (clearing immersion NA = 1.0). The acquisition mode settings we most commonly use are as follows: scan mode = frame, frame size = 1,024 × 1,024, averaging number = 1, bit depth = 8. Activate the *z*-stack mode (define lower and upper limits) and multi-view mode (×4). Set the light-sheet thickness to ~6 µm and use dual illumination.

(ii) Use the 3D view tab in the Arivis imaging software to optimize brightness, contrast and 3D-rendering properties for the best representation of the imaging. After corrections, the RGB images can be exported as TIFF files (>300 d.p.i. is recommended).

Troubleshooting

Troubleshooting advice can be found in Table 2.

Table 2 | Troubleshooting table

Step	Problem	Possible reason	Solution
3	Loss of organoids during the experiment	Organoids stuck to pipette tips or tubes	Carefully precoat the tubes and tips with 1% (wt/vol) PBS–BSA
8	Cystic organoids collapse during fixation	Suboptimal fixation conditions	Try a different fixative, such as formalin or 2% (vol/vol) PFA–glutaraldehyde
10	Loss of organoids during the experiment	Organoids stuck to 24-well plates	Make sure to use low-adherence/ suspension plates
20	Loss of organoids during the experiment	Organoids were aspirated while washing	Increase the time to allow the organoids to settle; remove the OWB more gently
24A(iii)	Cystic organoids appear folded after clearing	Organoid shrinkage during clearing	Skip clearing and image with multiphoton microscopy

Table continued

Table 2 (continued)

Step	Problem	Possible reason	Solution
25A(i)	Weak signal obtained using directly conjugated antibodies	Low amounts of epitope	Amplify the signal with a secondary antibody step
	Weak signal of fluorescent reporter	Fixation time was too long or too short The fluorescent reporter signal was weak initially	Optimize fixation time Perform immunolabeling of the fluorophore to amplify the signal
	Weak signal of immunolabeled nuclear proteins	Inefficient antibody penetration of the nucleus	Use OWB supplemented with 0.02% SDS (wt/vol)
25A(i, ii)	Organoids move while imaging (usually observed as suboptimal results after image stitching)	Suboptimal fixation of organoids between slide and coverslip Suboptimal fixation of slide on microscope	Use fewer layers of sticky tape during slide preparation Improve slide fixation to microscope

Timing

Steps 1–6, organoid recovery from 3D matrix: 1–1.5 h
Steps 7–11, fixation and blocking: 1 h
Steps 12–23, immunolabeling: 44 h
Step 24A(i–iii), sample preparation, clearing: 20 min
Step 24A(iv–ix), slide preparation for imaging: 15 min
Step 24B, sample preparation for light-sheet microscopy: 2–16 h
Step 25A, imaging and image processing for single-photon and multiphoton imaging: 1–2 h
Step 25B, imaging and image processing for light-sheet imaging: 40–90 min

Anticipated results

Imaging organoids in 3D opens new opportunities to visualize morphology, cell type composition and intracellular processes in detail in their 3D culture environment. This technique is simple and probably applicable to most organoid systems derived from different host species or organs.

The power of 3D imaging, as compared to 2D imaging, is demonstrated by images of a mouse mammary gland organoid generated using recently published methods[14]. These organoids contain a central layer of columnar-shaped $K8^+/K18^+$ luminal cells and an outer layer of elongated $K5^+$ basal cells (Fig. 4a), which is similar to their morphology in vivo[22]. It is difficult to appreciate this morphology on a 2D section of the same organoid (Fig. 4a, middle panel). Another example using human liver organoid culture methods[11] shows that 3D imaging is superior to 2D imaging for viewing the network of $MRP2^+$ canaliculi that facilitate the collection of bile fluid (Fig. 4b). These methods thus allow visualization of essential structural features of organoid specimens.

In addition to visualization of whole-mount organoids at cellular resolution, we combined organoid 3D imaging with the Airyscan Fast imaging module of the Zeiss LSM 880 confocal microscope to enable high-resolution imaging (120 nm of lateral and 350 nm of axial resolution, as compared with 250 and 800 nm for conventional confocal microscopy). For example, in a human airway organoid, the different stages of development of acetylated-tubulin$^+$ cilia can be seen at high resolution (Fig. 2b). This opens possibilities for studying intracellular processes, such as cytoskeleton remodeling or vesicle transport, in different types of organoids.

With the optical clearing step described above, organoids can be imaged with enhanced fluorescence intensity and increasing *z*-depth penetration as compared with those of a commercially available reagent, FocusClear, and uncleared sample (Fig. 3a–c). The resolution obtained allows cellular segmentation algorithms to quantify the number of cells and presence of different cell markers in different cellular subtypes in whole organoids. We present an example of an organoid containing 140 cells, in which 3 cells are highly positive for the Ki67 cell cycle marker (Fig. 4c).

In summary, the 3D imaging technique we describe here is simple, is reproducible and can provide volumetric data for immunolabeled organoids, as well as for organoids expressing fluorescent reporters, within 3 d. The protocol has been successfully applied to a broad range of organoids, including those of mouse or human origin, as well as healthy versus disease models. The sample

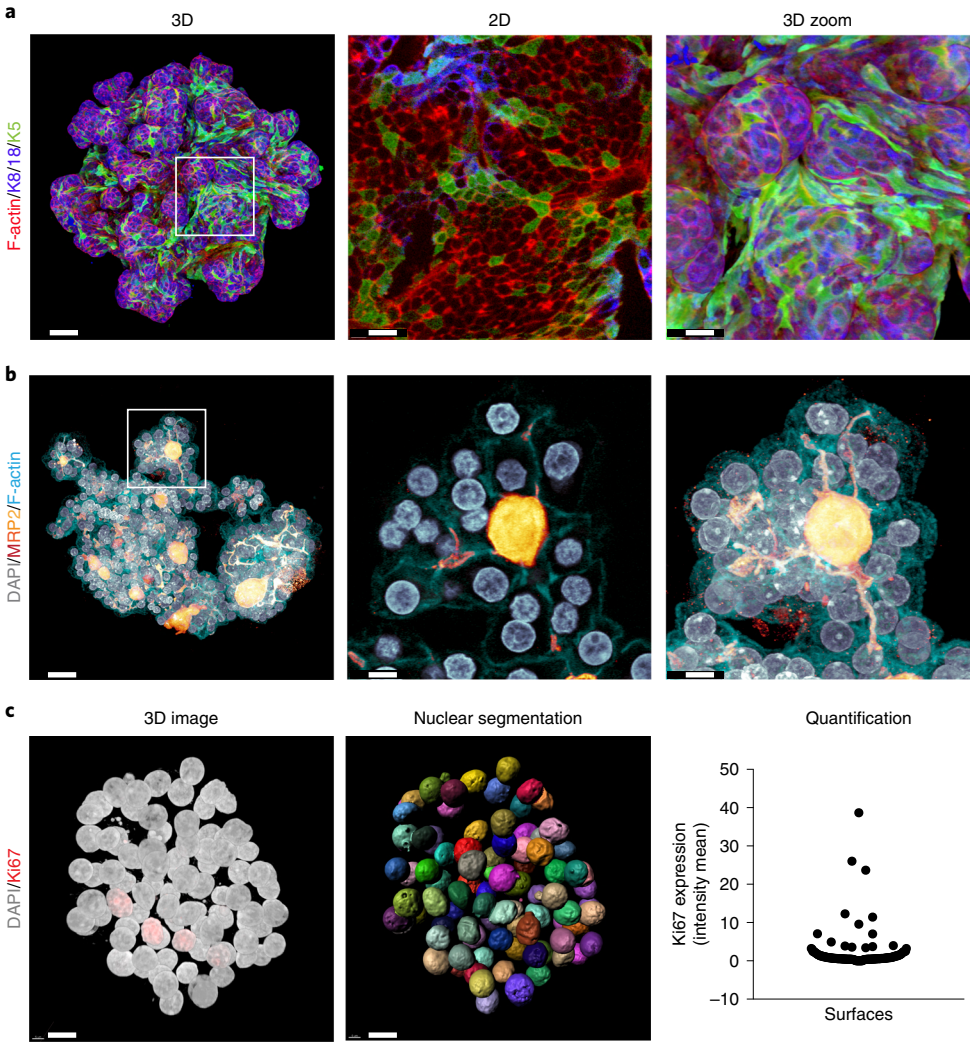

Fig. 4 | 3D imaging enables acquisition of accurate architectural information and 3D quantification. a,**b**, Confocal images representing whole-mount 3D images (left), 2D optical sections (middle) and 3D areas of an enlarged section (right) of an organoid derived from a single basal cell of the mouse mammary gland (**a**) labeled for K8/18 (blue), K5 (green) and F-actin (red) (fructose–glycerol clearing; 25× oil objective) or a human fetal liver organoid (**b**) labeled for DAPI (gray), MRP2 (yellow–red) and F-actin (blue) (fructose–glycerol clearing; 40× oil objective). The images illustrate the advantage of 3D imaging as compared with 2D sectioning to appreciate the morphology of elongated mammary basal cells that surround luminal cells (**a**, white square) or the network of MRP2-positive canaliculi (**b**, white square). Scale bars, 55 µm (**a**, left), 40 µm (**a**, middle and right), 25 µm (**b**, left), and 8 µm (**b**, middle and right). **c**, Confocal 3D whole-mount image of a human fetal liver organoid labeled with DAPI and Ki67 (left) and a segmented image on the DAPI channel generated using Imaris (middle). Scale bars, 15 µm. (Right) Graph plotted in GraphPad Prism 6 representing the Ki67 mean intensity in all the cells (DAPI-segmented) of the entire organoid (140 cells).

preparation is versatile and the samples can be imaged using confocal, multiphoton and light-sheet fluorescent microscopes to obtain cellular to subcellular resolution of intact organoids.

Reporting Summary

Further information on research design is available in the Nature Research Reporting Summary linked to this article.

Data availability

All data generated or analyzed during this study are included in this published article (and its supplementary information files).

References

1. Sato, T. & Clevers, H. SnapShot: growing organoids from stem cells. *Cell* **161**, 1700–1700.e1 (2015).
2. Clevers, H. Modeling development and disease with organoids. *Cell* **165**, 1586–1597 (2016).
3. Drost, J. & Clevers, H. Organoids in cancer research. *Nat. Rev. Cancer* **18**, 407–418 (2018).
4. Bartfeld, S. & Clevers, H. Stem cell-derived organoids and their application for medical research and patient treatment. *J. Mol. Med.* **95**, 729–738 (2017).
5. Broutier, L. et al. Human primary liver cancer-derived organoid cultures for disease modeling and drug screening. *Nat. Med.* **23**, 1424–1435 (2017).
6. Dekkers, J. F. et al. Characterizing responses to CFTR-modulating drugs using rectal organoids derived from subjects with cystic fibrosis. *Sci. Transl. Med.* **8**, 344ra384 (2016).
7. Dekkers, J. F. et al. A functional CFTR assay using primary cystic fibrosis intestinal organoids. *Nat. Med.* **19**, 939–945 (2013).
8. Sato, T. et al. Single Lgr5 stem cells build crypt-villus structures in vitro without a mesenchymal niche. *Nature* **459**, 262–265 (2009).
9. Karthaus, W. R. et al. Identification of multipotent luminal progenitor cells in human prostate organoid cultures. *Cell* **159**, 163–175 (2014).
10. Lancaster, M. A. et al. Cerebral organoids model human brain development and microcephaly. *Nature* **501**, 373–379 (2013).
11. Hu, H. et al. Long-term expansion of functional mouse and human hepatocytes as 3D organoids. *Cell* **175**, 1591–1606.e19 (2018).
12. Huch, M. et al. Long-term culture of genome-stable bipotent stem cells from adult human liver. *Cell* **160**, 299–312 (2015).
13. Nanki, K. et al. Divergent routes toward Wnt and R-spondin niche independency during human gastric carcinogenesis. *Cell* **174**, 856–869.e17 (2018).
14. Jamieson, P. R. et al. Derivation of a robust mouse mammary organoid system for studying tissue dynamics. *Development* **144**, 1065–1071 (2017).
15. Sachs, N. et al. A living biobank of breast cancer organoids captures disease heterogeneity. *Cell* **172**, 373–386. e10 (2018).
16. Turco, M. Y. et al. Long-term, hormone-responsive organoid cultures of human endometrium in a chemically defined medium. *Nat. Cell Biol.* **19**, 568–577 (2017).
17. Maimets, M. et al. Long-term in vitro expansion of salivary gland stem cells driven by Wnt signals. *Stem Cell Rep.* **6**, 150–162 (2016).
18. Ren, W. et al. Single Lgr5- or Lgr6-expressing taste stem/progenitor cells generate taste bud cells ex vivo. *Proc. Natl. Acad. Sci. USA* **111**, 16401–16406 (2014).
19. Richardson, D. S. & Lichtman, J. W. Clarifying tissue clearing. *Cell* **162**, 246–257 (2015).
20. Richardson, D. S. & Lichtman, J. W. SnapShot: tissue clearing. *Cell* **171**, 496–496.e1 (2017).
21. Rios, A. C. et al. Essential role for a novel population of binucleated mammary epithelial cells in lactation. *Nat. Commun.* **7**, 11400 (2016).
22. Rios, A. C., Fu, N. Y., Lindeman, G. J. & Visvader, J. E. In situ identification of bipotent stem cells in the mammary gland. *Nature* **506**, 322–327 (2014).
23. Rios, A. C. & Clevers, H. Imaging organoids: a bright future ahead. *Nat. Methods* **15**, 24–26 (2018).
24. Sachs, N. et al. Long-term expanding human airway organoids for disease modeling. *EMBO J.* **38**, e100300 (2019).
25. Shutgens, F. et al. Tubuloids derived from human adult kidney and urine for personalized disease modelling. *Nat. Biotechnol.* **37**, 303–313 (2019).
26. Eisenstein, M. Transparent tissues bring cells into focus for microscopy. *Nature* **564**, 147–149 (2018).
27. Erturk, A. et al. Three-dimensional imaging of solvent-cleared organs using 3DISCO. *Nat. Protoc.* **7**, 1983–1995 (2012).
28. Renier, N. et al. iDISCO: a simple, rapid method to immunolabel large tissue samples for volume imaging. *Cell* **159**, 896–910 (2014).
29. Kubota, S. I. et al. Whole-body profiling of cancer metastasis with single-cell resolution. *Cell Rep.* **20**, 236–250 (2017).
30. Murakami, T. C. et al. A three-dimensional single-cell-resolution whole-brain atlas using CUBIC-X expansion microscopy and tissue clearing. *Nat. Neurosci.* **21**, 625–637 (2018).
31. Susaki, E. A. et al. Whole-brain imaging with single-cell resolution using chemical cocktails and computational analysis. *Cell* **157**, 726–739 (2014).
32. Chung, K. et al. Structural and molecular interrogation of intact biological systems. *Nature* **497**, 332–337 (2013).
33. Tomer, R., Ye, L., Hsueh, B. & Deisseroth, K. Advanced CLARITY for rapid and high-resolution imaging of intact tissues. *Nat. Protoc.* **9**, 1682–1697 (2014).
34. Snippert, H. J. et al. Intestinal crypt homeostasis results from neutral competition between symmetrically dividing Lgr5 stem cells. *Cell* **143**, 134–144 (2010).
35. Stelzer, E. H. Light-sheet fluorescence microscopy for quantitative biology. *Nat. Methods* **12**, 23–26 (2015).
36. Huisken, J., Swoger, J., Del Bene, F., Wittbrodt, J. & Stelzer, E. H. Optical sectioning deep inside live embryos by selective plane illumination microscopy. *Science* **305**, 1007–1009 (2004).

Acknowledgements

We are very grateful for the technical support from the Princess Máxima Center for Pediatric Oncology and to the Hubrecht Institute and Zeiss for imaging support and collaborations. All the imaging was performed at the Princess Máxima imaging center. This work was financially supported by the Princess Máxima Center for Pediatric Oncology. J.F.D. was supported by a Marie Curie Global Fellowship and a VENI grant from the Netherlands Organisation for Scientific Research (NWO). J.E.V. was supported by the Australian National Health and Medical Research Council (NHMRC).

Author contributions

J.F.D. designed the study, performed experiments and interpreted data; J.F.D., M.A., L.M.W., H.C.R.A. and P.R.J. performed experiments and analyzed data; J.F.D., P.R.J., A.M.V., G.D.A., H.H. and J.M.B. performed the organoid culturing. K.C.O. and H.J.G.S. provided fluorescent constructs; A.C.R. helped design the study and carried out data interpretation; J.F.D. and A.C.R. cowrote the manuscript. J.E.V., H.C. and E.J.W. helped with data interpretation, manuscript writing and corrections.

Competing interests

H.C. is named as inventor on several patents related to organoid technology. J.F.D. is named as inventor on one patent related to the organoid technology.

Additional information

Supplementary information is available for this paper at https://doi.org/10.1038/s41596-019-0160-8.

Reprints and permissions information is available at www.nature.com/reprints.

Correspondence and requests for materials should be addressed to A.C.R.

Journal peer review information: *Nature Protocols* thanks Xavier Gidrol, Melissa Skala and other anonymous reviewer(s) for their contribution to the peer review of this work.

Publisher's note: Springer Nature remains neutral with regard to jurisdictional claims in published maps and institutional affiliations.

Received: 13 December 2018; Accepted: 4 March 2019;
Published online: 3 May 2019

Related links

Key references using this protocol

Hu, H. et al. *Cell* **175**, 1591–1606.e19 (2018): https://doi.org/10.1016/j.cell.2018.11.013

Sachs, N. et al. *EMBO J.* **38**, e100300 (2019): https://doi.org/10.15252/embj.2018100300

nature research

Corresponding author(s): Anne Rios NP-P180819A

Last updated by author(s): Jan 27, 2019

Reporting Summary

Nature Research wishes to improve the reproducibility of the work that we publish. This form provides structure for consistency and transparency in reporting. For further information on Nature Research policies, see Authors & Referees and the Editorial Policy Checklist.

Statistics

For all statistical analyses, confirm that the following items are present in the figure legend, table legend, main text, or Methods section.

n/a	Confirmed
☒	☐ The exact sample size (*n*) for each experimental group/condition, given as a discrete number and unit of measurement
☐	☒ A statement on whether measurements were taken from distinct samples or whether the same sample was measured repeatedly
☐	☒ The statistical test(s) used AND whether they are one- or two-sided *Only common tests should be described solely by name; describe more complex techniques in the Methods section.*
☒	☐ A description of all covariates tested
☐	☒ A description of any assumptions or corrections, such as tests of normality and adjustment for multiple comparisons
☐	☒ A full description of the statistical parameters including central tendency (e.g. means) or other basic estimates (e.g. regression coefficient) AND variation (e.g. standard deviation) or associated estimates of uncertainty (e.g. confidence intervals)
☐	☒ For null hypothesis testing, the test statistic (e.g. *F*, *t*, *r*) with confidence intervals, effect sizes, degrees of freedom and *P* value noted *Give P values as exact values whenever suitable.*
☒	☐ For Bayesian analysis, information on the choice of priors and Markov chain Monte Carlo settings
☒	☐ For hierarchical and complex designs, identification of the appropriate level for tests and full reporting of outcomes
☒	☐ Estimates of effect sizes (e.g. Cohen's *d*, Pearson's *r*), indicating how they were calculated

Our web collection on statistics for biologists contains articles on many of the points above.

Software and code

Policy information about availability of computer code

Data collection	Zen black, microscope software for Zeiss dual platform confocal/multiphoton 880 and light sheet Z.1. Imaris software (Bitplane) version 8.2.1 was used for 3D and 3D stereo visualization and segmentation of confocal and multiphoton data. Surfaces module was used for threshold based segmentation. For each segmented cell measurements of channel intensity were extracted.
Data analysis	GraphPad Prism 6 was used for segmented cell analysis and plotting.

For manuscripts utilizing custom algorithms or software that are central to the research but not yet described in published literature, software must be made available to editors/reviewers. We strongly encourage code deposition in a community repository (e.g. GitHub). See the Nature Research guidelines for submitting code & software for further information.

Data

Policy information about availability of data

All manuscripts must include a data availability statement. This statement should provide the following information, where applicable:

- Accession codes, unique identifiers, or web links for publicly available datasets
- A list of figures that have associated raw data
- A description of any restrictions on data availability

All data generated or analysed during this study are included in this published article (and its supplementary information files)

Field-specific reporting

Please select the one below that is the best fit for your research. If you are not sure, read the appropriate sections before making your selection.

☒ Life sciences ☐ Behavioural & social sciences ☐ Ecological, evolutionary & environmental sciences

For a reference copy of the document with all sections, see nature.com/documents/nr-reporting-summary-flat.pdf

Life sciences study design

All studies must disclose on these points even when the disclosure is negative.

Sample size	Depending on the organoid size and origin and due to potential loss during the sample preparation, we ideally start the experiment with 50-200 organoids for confocal or multi-photon imaging and 100-200 organoids for light sheet imaging to obtain enough organoids for imaging experiment (usually 10-20 organoids were imaged per experiments and the remaining frozen down).
Data exclusions	No data exclusion.
Replication	10-20 organoids were analyzed per experiment (replicated at least 2 times). All replications were successful.
Randomization	Randomization is not relevant to our study since we describe a protocol of sample preparation for 3D imaging of all types of organoid.
Blinding	Blinding is not relevant to our study since we describe a protocol of sample preparation for 3D imaging of all type of organoid.

Reporting for specific materials, systems and methods

We require information from authors about some types of materials, experimental systems and methods used in many studies. Here, indicate whether each material, system or method listed is relevant to your study. If you are not sure if a list item applies to your research, read the appropriate section before selecting a response.

Materials & experimental systems

n/a	Involved in the study
☐	☒ Antibodies
☒	☐ Eukaryotic cell lines
☒	☐ Palaeontology
☐	☒ Animals and other organisms
☐	☒ Human research participants
☒	☐ Clinical data

Methods

n/a	Involved in the study
☒	☐ ChIP-seq
☒	☐ Flow cytometry
☒	☐ MRI-based neuroimaging

Antibodies

Antibodies used	Table 1
Validation	All antibodies used are commercialized and have been previously tested. Information is included in table 1

Animals and other organisms

Policy information about studies involving animals; ARRIVE guidelines recommended for reporting animal research

Laboratory animals	organoids from FVB/N mouse Female 6-10-week-old
Wild animals	*Provide details on animals observed in or captured in the field; report species, sex and age where possible. Describe how animals were caught and transported and what happened to captive animals after the study (if killed, explain why and describe method; if released, say where and when) OR state that the study did not involve wild animals.*
Field-collected samples	*For laboratory work with field-collected samples, describe all relevant parameters such as housing, maintenance, temperature, photoperiod and end-of-experiment protocol OR state that the study did not involve samples collected from the field.*
Ethics oversight	All animal experiments conform to regulatory standards and were approved by the Walter and Eliza Hall Institute (WEHI) Animal Ethics Comittee.

Note that full information on the approval of the study protocol must also be provided in the manuscript.

Human research participants

Policy information about studies involving human research participants

Population characteristics	Human airways, kidney, liver, breast cancer and CF (Cystic fibrosis) organoids.
Recruitment	All human organoids samples were obtained from biobanks through Hubrecht Organoid Technology (HUB, www.hub4organoids.nl).
Ethics oversight	Authorizations were obtained by the ethical committee UMC Utrecht (METC UMCU) at request of the HUB in order to ensure compliance with the Dutch medical research involving human subjects' act and informed consent was obtained from donors when appropriate.

Note that full information on the approval of the study protocol must also be provided in the manuscript.